2021 43rd Annual International Conference of the
IEEE Engineering in Medicine & Biology Society (EMBC)
Oct 31 - Nov 4, 2021. Virtual Conference

Seizure Onset Zone Identification Based on Phase-Amplitude Coupling of Interictal Electrocorticogram

Yao Miao[1], Yasushi Iimura[2], Hidenori Sugano[2], Kosuke Fukumori[1], Taku Shoji[1], and Toshihisa Tanaka[1,2,3,4,5]

***Abstract*— Presurgical localization from interictal electrocorticogram (ECoG) and resection of seizure onset zone (SOZ) are difficult processes to achieve seizure freedom. Recently, high frequency oscillations (HFOs) have been recognized as reliable biomarkers for epilepsy surgery which has a relation with the phase of low frequency activities in ECoG. Considering the recent valid biomarker for epilepsy surgery, we hypothesize that the approach of coupling between HFOs and low frequency phases differs SOZ from non-seizure onset zone (NSOZ). This study proposes phase-amplitude coupling (PAC) method to identify SOZ by measuring whether the amplitude of HFOs is coupled with a phase at 2–34 Hz in ECoG. Besides, three machine learning models for PAC-based features are designed for SOZ detection. Four patients with focal cortical dysplasia (FCD) are examined to observe efficiency. Experimental results indicate that the mode of coupling is a potential feature to detect SOZ.**

***Clinical relevance*— This suggests the PAC feature between low frequency phase and HFO amplitude may be used as a candidate biomarker to detect SOZ.**

I. INTRODUCTION

Epilepsy is one of the most common neurological disorders, with a prevalence of about 65 million people throughout the world, as well as a rate between 0.4% and 1% of people who have active seizures worldwide at any time [1]–[3]. Electroencephalography (EEG) is one of the most important tools for diagnosing epilepsy. In particular, for focal epilepsy treatment, the identification of the seizure onset zone (SOZ) from intracranial EEG (electrocorticogram: ECoG) is crucial for a surgery to resect an area where seizures originate.

To identify the SOZ from EEG/ECoG signals, the PAC method is one of the most important forms, which reflects relevant diagnose information by measuring the coupling between the amplitude of high frequency oscillations (HFOs) and the phase of low frequency activities in EEG/ECoG signals. Recently, this coupling between the HFOs and the phase of low frequency activities has been considered a promising biomarker to detect the seizure onset zone (SOZ). Varatharajah et al. [4] observed that prominent coupling existed in interictal ECoG of SOZ. Amiri et al. [5] demonstrated that the PAC of interictal EEG was stronger in SOZ compared to normal zone within the frequency range less than 260 Hz. Motoi et al. [6] revealed that the PAC could be as the biomarker of SOZ detection from interictal ECoG data. Their study reported that the difference of PAC values was obvious between the ripple amplitude and the phase of slow-wave (3–4 Hz). Other studies with intracranial electroencephalography (iEEG) signals also demonstrated that the dynamic modulation of epileptic high frequency amplitude was most significantly modulated by the phase of slower cortical rhythms [7], [8]. However, the existing studies with the PAC method to detect the SOZ from interictal EEG/ECoG signals used interictal EEG/ECoG signals consisting of only frequency bands with frequency ranges 0.5–300 Hz. Besides, recent findings in neurology have illustrated that the HFOs including ripple (80–250 Hz) and fast ripple (250–600 Hz) are the valid biomarkers to guide epilepsy surgery [9]–[11].

Recent clinical findings [12]–[14] motivated the present paper to detect SOZ based on the coupling relationship between the low frequency and high frequency (ripple and fast ripple) bands. We hypothesize that PAC between HFOs amplitude and low frequency phases differ between SOZ and non-seizure onset zone (NSOZ). Our analysis focused on the difference of the PAC between the phase of different sub-bands at 2–34 Hz and the amplitude of different sub-bands in high frequency (80–560 Hz). Statistical analysis and machine learning approaches were employed to evaluate the differences.

II. METHODS

A. Subjects and ECoG Recordings

The dataset in this paper was from epileptic patients who underwent monitoring by implanting with electrodes at Juntendo University Hospital in Japan between October, 2016 and July, 2018. The study was approved by Juntendo University Hospital and the Tokyo University of Agriculture and Technology Ethics Committee. All patients gave written informed consent for the research purpose of their ECoG data.

Four patients (three males and one female) with the focal cortical dysplasia (FCD) type 2B and with outcome of seizure free after epilepsy surgery, at ages of a range from 15 to 39 were selected. For each patient, electrodes for continuous one hour of ECoG during interictal periods were chosen, with a sampling frequency of 2,000 Hz. Among

*This work was fully funded by JST CREST (Grant No. JPMJCR1784). (Corresponding author: Toshihisa Tanaka.)

[1]Y. Miao, K. Fukumori, and T. Shoji are with Tokyo University of Agriculture and Technology, 2–24–16 Nakacho, Koganei-shi, Japan

[2]Y. Iimura and H. Sugano are with the Department of Neurosurgery, Juntendo University, Tokyo, Japan

[1,2,3,4,5]T. Tanaka is with Tokyo University of Agriculture and Technology, 2–24–16 Nakacho, Koganei-shi, Japan, and the Department of Neurosurgery, Juntendo University, Tokyo, Japan, and RIKEN Center for Brain Science, Saitama, Japan, and RIKEN Center for Advanced Intelligent Project, Tokyo, Japan, and Hangzhou Dianzi University, Hangzhou, China. tanakat@cc.tuat.ac.jp

these electrodes, electrodes in SOZ and the rest were labeled as SOZ and NSOZ by experts, where the numbers of SOZ electrode for four patients are 7, 10, 10, and 16, respectively, and the corresponding numbers of NSOZ electrode are 63, 60, 40, and 60, respectively.

B. Analysis Based on PAC

To investigate the coupling in the SOZ, the PAC was employed. PAC is explained as that the high frequency amplitude is modulated by the low frequency phase. The whole PAC analysis process is illustrated in Fig. 1.

1) Preprocessing: The discrete interictal ECoG signal denoted by $s(n)$ with a duration of an hour was filtered into a total of 32 sub-bands, including 16 sub-bands in the low frequency range (2–34 Hz) with 2 Hz bandwidth, as well as 16 sub-bands in the high frequency range (80–560 Hz) in which the bandwidth was set to 30 Hz. Filtered components are denoted by $s^i_{pha}(n)$ $(i = 1, 2, \ldots, 16)$ and $s^j_{amp}(n)$ $(j = 1, 2, \ldots, 16)$ for low and high frequency parts, respectively. Filtering was performed by the finite impulse response (FIR), where the scipy.signal.firwin function introduced from Python was applied with the length of the filter was set to odd to avoid zero response at the Nyquist frequency. In detail, the Kaiser window was used in the filter and the desired attenuation in the stopband was set to 60 dB. It should be emphasized that compared to the frequency range (0.5–300 Hz) of bandpass filtering from the previous studies illustrated above, our work firstly extended the filtering range of the dataset to 560 Hz, including the fast ripple band (250–600 Hz) of HFO.

2) PAC Between High and Low Frequency Components: The mean vector length modulation index (MVL-MI) [15] was employed to evaluate PAC. Four steps were included to computation of MVL-MI as follows:

- For complex analytic signal $z(n)$, which is either $s^i_{pha}(n)$ or $s^j_{amp}(n)$, the polar coordinate is defined as

$$z(n) = a_{amp}(n)e^{i\varphi_{pha}(n)}(n = 1, 2, \ldots, N), \quad (1)$$

  where $a_{amp}(n)$ is the amplitude at high frequency band and $\varphi_{pha}(n)$ is the phase at low frequency band.
- Define the Modulation Index (MI) value of $z(n)$, MI_{raw}, which is calculated by taking the absolute value of mean vector of $z(n)$ as

$$MI_{raw} = \left| \frac{1}{N} \sum_{n=1}^{N} \boldsymbol{z}(n) \right| (n = 1, 2, \ldots, N). \quad (2)$$

- The surrogate data approach is used to compute the surrogate $z_s(n)(n = 1, 2, \ldots, N; s = 1, 2, \ldots, S)$ by introducing an arbitrary time lag between $\varphi_{pha}(n)$ and $a_{amp}(n)$. Then, the MI value of $z_s(n)$ is calculated as

$$MI_s = \left| \frac{1}{N} \sum_{n=1}^{N} \boldsymbol{z}_s(n) \right| (n = 1, 2, \ldots, N; s = 1, 2, \ldots, S). \quad (3)$$

- With mean μ and standard deviation σ of the surrogate $MI_s(s = 1, 2, \ldots, S)$, calculate the normalized MI as

$$MI = \frac{MI_{raw} - \mu}{\sigma}, \quad (4)$$

  which is used to evaluate the PAC strength.

3) Phase-Amplitude Comodulogram: Phase-amplitude comodulogram is a graphical display, which is employed to present a series of PAC values over a grid of frequencies [16], [17]. It is used to locate initially the frequency where coupling occurs in case of there is no prior assumption of the frequency of phase-modulating and amplitude-modulated. As shown in the rightmost sub-figure of Fig. 1, the frequency of phase and amplitude are displayed in the horizontal axis and ordinate axis, respectively. Each point of comodulogram is the MI value at (i, j), which is exhibited by using a pseudocolor plot with hot color denoting strong coupling.

C. Classifier

Since each segment of phase-amplitude comodulogram can be converted into an image with 16×16 pixels. In this study, we use support vector machines (SVMs) and a 2-D CNN structure for classification based on comodulogram results obtained. We propose the 2-D CNN model consisting of three convolutional layers and two fully connected layers, as illustrated in Fig. 2. Each convolutional layer consists of the 'He Uniform' initialization, a rectified linear unit (ReLU) activation, and batch normalization. The former fully connected layer has a ReLU activation while the latter has a sigmoid activation. Besides, the focal loss function is introduced in this model to address the imbalanced classification. It is a modulating term of cross-entropy (CE) loss function, which makes the model focus training on hard samples by down-weighting of easy samples [18]. SVMs are supervised learning models by creating hyperplane in feature space to separate inputs into classes, which consists of different kernel functions for classification. In this study, the radial basis function (RBF) kernel and linear kernel are employed.

III. Results

To analysis with PAC approach, one hour interictal ECoG with 20 seconds per segment for four patients was used for evaluation. The low frequency (2–34 Hz) and HFOs (80–560 Hz) for each segment of each channel were decomposed with 2 Hz and 30 Hz bandwidth, respectively, yielding 16 and 16 sub-bands each. The PAC values were estimated by coupling with the phase of each sub-band of low frequency and the sub-bands of high frequency amplitude.

A. Results of Statistical Analysis

To examine the significance of PAC values between SOZ and NSOZ, the Mann-Whitney U test was performed to PAC values at each of the band pairs ($\delta - HFO$, $\theta - HFO$, $\alpha - HFO$, and $\beta - HFO$) for SOZ and NSOZ. As shown in Fig. 3, the results of Mann-Whitney U test showed that the PAC values distribution of SOZ is significantly different when compared to NSOZ at four band pairs for four patients at a significant level of 0.01. Besides, the median PAC value

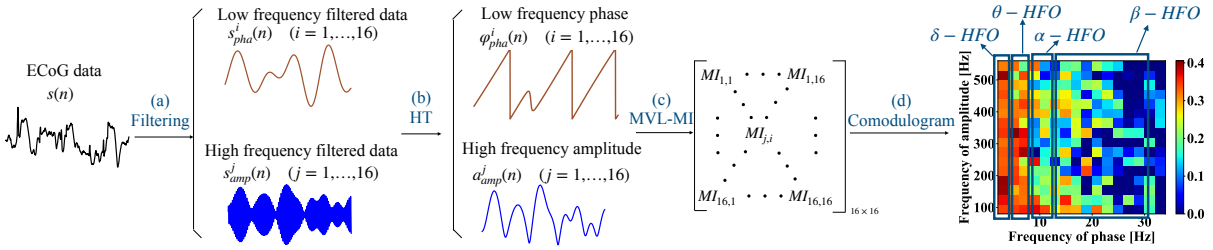

Fig. 1. The scheme of PAC analysis for ECoG. $s(n)$ denotes the raw ECoG data. $\varphi^i_{pha}(n)$ and $a^j_{amp}(n)$ are the phase at low frequency and amplitude at high frequency which are calculated from $s^i_{pha}(n)$ and $s^j_{amp}(n)$ by using Hilbert transform (HT), respectively. $\theta - HFO$ indicates the corresponding a band pair when computing PAC values, in which the first band is the band of phase with locating in x-axis, as well as the second band is the band of amplitude with setting in y-axis. δ, θ, α, β, and HFO are the frequency bands of (2–4 Hz), (4–8 Hz), (8–12 Hz), (13–30 Hz), and (80-560 Hz), respectively. The parts surrounded by blue rectangle show the array of PAC values at the designated band pair.

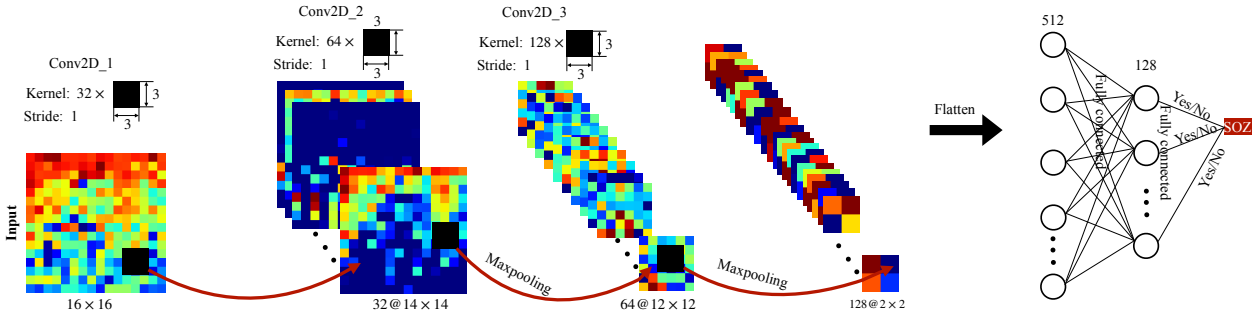

Fig. 2. The architecture of the proposed 2D CNN model. Comodulogram with the size of 16×16 of raw ECoG recordings is used as input. There are three convolutional layers named as $Con2D\_1$, $Con2D\_2$, and $Con2D\_3$, respectively. Each convolutional layer consists of a 'He Uniform' initialization, a ReLU activation function, and a batch normalization. The kernel size and the stride value for all three convolutional layers are the same, which is 3×3 and 1, respectively. For $Con2D\_1$, there are 32 kernels. For $Con2D\_2$, there are 64 kernels. The following is MaxPooling with a size of 2×2. For $Con2D\_3$, there are 128 kernels. Following is also MaxPooling with the same size as before. Features extracted by three convolutional layers are flattened and connected by two fully connected layers with an output size of 128 and 1, respectively. A ReLU activation and a sigmoid activation are applied for the former and the latter fully connected layer, respectively. Besides, the former fully connected layer consists of a dropout rate of 0.5.

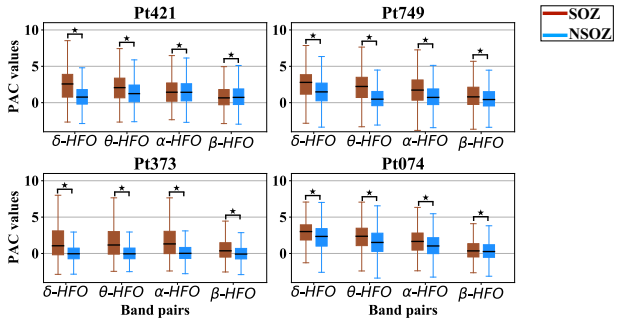

Fig. 3. Mann-Whitney U test results of SOZ and NSOZ group at four band pairs for four patients. Brown color and blue color denotes SOZ and NSOZ, respectively. X-axis indicates the type of band pairs, which consists of four types of band pairs. Y-axis denotes the PAC value. $\star$ denotes $p < 0.01$.

of SOZ was higher than PAC values of NSOZ at the band pairs of $\delta - HFO$, $\theta - HFO$, and $\alpha - HFO$ for four patients.

B. Results of Classification

Three classifiers (2D-CNN, SVM with linear kernel, and SVM with RBF kernel) illustrated above were applied for SOZ identification. To obtain a lower bias evaluation, the time series cross-validation (CV) was used with the number of the split set to five [19]. The area under the curve (AUC) is used to evaluate classification results. As illustrated in Table I, the average AUC in a band pair of $(2-34\,\text{Hz}) - HFO$ using CNN, SVM with linear kernel, and SVM with RBF kernel were 0.87, 0.88, and 0.90, respectively. The averaged AUC of SVM with RBF kernel was the best among the three. Besides, the AUC of four patients (Pt421, Pt749, Pt373, and Pt074) was higher than 0.8 using all three classifiers. Moreover, as shown in Table II, the averaged AUCs in a band pair of $(2-34\,\text{Hz}) - (80-300\,\text{Hz})$ based on the same SVM models were 0.84 and 0.90, respectively, which were

TABLE I
AUC IN BAND PAIR OF $(2-34\,\text{Hz}) - HFO$ USING THREE CLASSIFIERS.

Patient	Pt421	Pt749	Pt373	Pt074	Average
CNN	0.93	0.92	0.82	0.81	0.87
SVM (Linear)	0.91	0.92	0.86	0.82	0.88
SVM (RBF)	0.94	0.94	0.85	0.85	0.90

TABLE II
AUC IN BAND PAIR OF $(2-34\,\text{Hz}) - (80-300\,\text{Hz})$ USING SVM.

Patient	Pt421	Pt749	Pt373	Pt074	Average
SVM (Linear)	0.83	0.85	0.86	0.82	0.84
SVM (RBF)	0.91	0.92	0.85	0.83	0.88

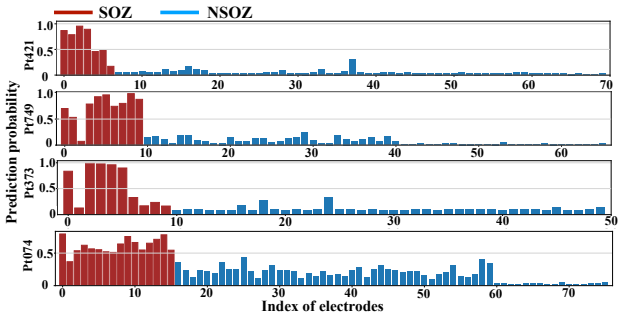

Fig. 4. Prediction probability bar in a band pair of $(2-34\,\mathrm{Hz})-HFO$.

lower than the results in a band pair of $(2-34\,\mathrm{Hz})-HFO$. Furthermore, the mean probability prediction in a band pair of $(2-34\,\mathrm{Hz})-HFO$ for each electrode was calculated to demonstrate the probability that the electrode was classified to be SOZ based on the SVM with RBF kernel. It was illustrated in Fig. 4 that for Pt421, Pt749, Pt373, and Pt074, six out of seven SOZ electrodes, nine out of ten SOZ electrodes, five out of ten SOZ electrodes, as well as 15 out of 16 SOZ electrodes could be detected with the probability prediction value higher than the NSOZ electrodes, respectively.

IV. Discussion and Conclusion

We investigate PAC of interictal ECoG for SOZ and NSOZ from four epilepsy patients by employing PAC approach (MVL-MI), statistical analysis method, and machine learning measures. We observe that a) there exists significant coupling between the phase of (2–34 Hz) and HFOs amplitude for SOZ when compared to NSOZ, b) SVM with RBF kernel is the best with the average AUC of 0.90 for SOZ detection among three classifiers, and c) the average AUC in a band pair of $(2-34\,\mathrm{Hz})-HFO$ is higher than that in a band pair of $(2-34\,\mathrm{Hz})-(80-300\,\mathrm{Hz})$. All three observations support the hypothesis illustrated in Section I. PAC is one type of brain wave synchronization. It is assumed to prompt effective interactions between neurons with similar phase preferences. Higher PAC values for the SOZ may be explained by the neuronal synchrony [20], [21].

The related studies on PAC analysis of ECoG for epileptic patients have illustrated that there is a strong coupling for ECoG during the interictal state in SOZ between low frequency phase and high frequency amplitude when compared in NSOZ [5], [6]. However, the maximum high frequency was limited to 300 Hz. Our findings firstly reveal that there was significant coupling between phase of low frequency and amplitude of HFOs for interictal ECoG in SOZ.

However, there are two major limitations in this study that could be addressed in future research. The first limitation is the small number of patients. To explain the generalization of the results illustrated above, a larger sample size of epileptic patients would be warranted. Another limitation of this research had to do with the singleness of features. It was shown in Table I that the SOZ region of Pt421 and Pt749 could be predicted well with a higher AUC of 0.94 using PAC alone, respectively, while the AUC for Pt373 and Pt074 was less than 0.9 by only applying PAC. It was encouraged to further improve the results in conjunction with other promising features in future research.

In conclusion, we have demonstrated that there was significant coupling between low frequency phase and amplitude of HFOs for interictal ECoG in SOZ using PAC approach. Besides, we employed three machine learning approaches to evaluate the effectiveness of PAC features for SOZ detection. The results suggest that PAC can be used as a potential feature for an automated detection of SOZ.

References

[1] G. Giannakakis, et al., "Methods for seizure detection and prediction: An overview," *Neuromethods*, vol. 91, pp. 131–157, 2014.

[2] M. Lévesque, et al., "High-frequency oscillations and mesial temporal lobe epilepsy," *Neuroscience Letters*, vol. 667, pp. 66–74, 2018.

[3] C. E. Stafstrom and L. Carmant, "Seizures and epilepsy: An overview for neuroscientists," *Cold Spring Harbor Perspectives in Medicine*, vol. 5, 2015.

[4] Y. Varatharajah, et al., "Integrating artificial intelligence with real-time intracranial EEG monitoring to automate interictal identification of seizure onset zones in focal epilepsy," *Journal of Neural Engineering*, vol. 15, 2018.

[5] M. Amiri, B. Frauscher, and J. Gotman, "Phase-amplitude coupling is elevated in deep sleep and in the onset zone of focal epileptic seizures," *Frontiers in Human Neuroscience*, vol. 10, 2016.

[6] H. Motoi, et al., "Phase-amplitude coupling between interictal high-frequency activity and slow waves in epilepsy surgery," *Epilepsia*, vol. 59, pp. 1954–1965, 2018.

[7] G. M. Ibrahim, et al., "Dynamic modulation of epileptic high frequency oscillations by the phase of slower cortical rhythms," *Experimental Neurology*, vol. 251, pp. 30–38, 2014.

[8] S. Samiee, et al., "Phase-amplitude coupling and epileptogenesis in an animal model of mesial temporal lobe epilepsy," *Neurobiology of Disease*, vol. 114, pp. 111–119, 2018.

[9] J. Jacobs, et al., "High-frequency electroencephalographic oscillations correlate with outcome of epilepsy surgery," *Annals of Neurology*, vol. 67, pp. 209–220, 2010.

[10] T. Fedele, et al., "Resection of high frequency oscillations predicts seizure outcome in the individual patient," *Scientific Reports*, vol. 7, 2017.

[11] B. Frauscher, et al., "High-frequency oscillations: The state of clinical research," *Epilepsia*, vol. 58, pp. 1316–1329, 2017.

[12] J. Jacobs, et al., "Interictal high-frequency oscillations (80–500 Hz) are an indicator of seizure onset areas independent of spikes in the human epileptic brain," *Epilepsia*, vol. 49, pp. 1893–1907, 2008.

[13] M. Dümpelmann, et al., "Automatic 80–250 Hz "ripple" high frequency oscillation detection in invasive subdural grid and strip recordings in epilepsy by a radial basis function neural network," *Clinical Neurophysiology*, vol. 123, 2012.

[14] K. Kerber, et al., "Differentiation of specific ripple patterns helps to identify epileptogenic areas for surgical procedures," *Clinical Neurophysiology*, vol. 125, 2014.

[15] R. T. Canolty, et al., "High gamma power is phase-locked to theta oscillations in human neocortex," *Science*, vol. 313, pp. 1626–1628, 2006.

[16] A. B. L. Tort, et al., "Measuring phase-amplitude coupling between neuronal oscillations of different frequencies," *Journal of Neurophysiology*, vol. 104, pp. 1195–1210, 2010.

[17] D. C. C. Lu, et al., "Realtime phase-amplitude coupling analysis of micro electrode recorded brain signals," *PLoS One*, vol. 13, 2018.

[18] T. Y. Lin, et al., "Focal loss for dense object detection," *2017 IEEE International Conference on Computer Vision (ICCV)*, pp. 2999–3007, 2017.

[19] C. Bergmeir and J. M. Benítez, "On the use of cross-validation for time series predictor evaluation," *Information Sciences*, vol. 191, pp. 192–213, 2012.

[20] E. B. Bromfield, et al., "Basic mechanisms underlying seizures and epilepsy," *West Hartford (CT): American Epilepsy Society*, 2006.

[21] E. A. Allen, et al., "Components of cross-frequency modulation in health and disease," *Frontiers in Systems Neuroscience*, vol. 5, 2011.